Journal of Applied Sciences

ISSN 1812-5654

science alert

ANSInet
an open access publisher
http://ansinet.com

Journal of Applied Sciences 9 (11): 2078-2087, 2009
ISSN 1812-5654

Investigation of Jet Break-Up Process in Diesel Engine Spray Modelling

[1]M.H. Djavareshkian and [2]A. Ghasemi
[1]Department of Mechanical Engineering, Ferdowsi University of Mashhad, Mashhad, Iran
[2]Department of Mechanical Engineering, University of Tabriz, Tabriz, Iran

Abstract: The objective of this study, is to simulate spray flow with different break-up models and investigate the processes of spray breakup and mixture formation. Effect of these models on the DI diesel engine combustion and performance is also investigated. The 3 Dimensional Naiver-Stokes equation is solved with SIMPLEC algorithm. An eddy break-up combustion model and a diesel auto-ignition model were implemented to simulate the ignition and combustion process in a diesel engine. All the simulations were carried out by the use of FIRE CFD tool. Results were validated via., available experimental data for OM_355 DI diesel engine for mean cylinder pressure. The results show that there have been good agreements between experiments and the CFD calculations. The research demonstrated that practically all the break-up models are capable of simulating the spray processes, as long as model constants are properly chosen and they affect the combustion simulation results.

Key words: Droplet, sauter mean diameter, penetration, coalescence

INTRODUCTION

In the last decade 3D-CFD has been successfully established for three dimensional simulations of fluid flow, mixture formation, combustion and pollutant formation in internal combustion engines. In direct injected engines the accuracy of the simulation results and hence their contribution to design analysis and optimization strongly depends on the predictive capabilities of the models adopted for simulation of the injector flow, spray formation and propagation characteristics (Tatschl and Riediger, 1998; Tatschl *et al*., 1998, 2000).

Since, experiments can be difficult to manage for injection conditions (small-scaled, high-speed flow), a numerical simulation seems to be an appropriate tool to get an interesting model of the flow features inside and at the exit of the injector nozzle. The knowledge of the injector mass flow rate and the flow conditions at the nozzle exit can be a key issue for a successful simulation of all the subsequent processes of mixture formation and eventually combustion and pollutant formation (Ueki *et al*., 2005). The diesel spray model must perform well for the proper prediction of the entire diesel combustion process. The quality of spray simulation could be judged by comparing global and local spray quantities with those obtained experimentally. Such global quantities comprise spray penetration, spray width and spray angle. Spray simulations involve multi-phase flow phenomena and as such require the numerical solution of conservation equations for the gas and the liquid phase simultaneously. With respect to the liquid phase, practically all spray calculations in the engineering environment today are based on a statistical method referred to as the Discrete Droplet Method (DDM) (Dukowicz, 1980).

Primary/secondary break-up modeling that accounts for the competing effects of turbulence, cavitation and aerodynamic induced break-up processes is based upon the spatially and temporally resolved injector flow data at the nozzle exit. The turbulence induced break-up is accounted for by solving a transport equation for the turbulent kinetic energy and its dissipation rate within the liquid fuel core (Naber and Reitz, 1988). The impact of the collapsing cavitation bubbles on the primary break-up is modeled via., additional source terms in the turbulence model. The turbulence and cavitation induced break-up competes with the aerodynamic one until at a certain distance downstream of the nozzle exit the aerodynamic break-up processes become dominant (Naber and Reitz, 1988). Due to dissipation of the turbulent fluctuations, however, the turbulence induced break-up rate is significantly reduced with increasing distance from the nozzle exit until it becomes negligible at about 2.5 mm downstream of the nozzle tip. The aerodynamic break-up rates show the opposite behavior, i.e., they are very low immediately at the nozzle exit but increase significantly with increasing distance from the nozzle, where the compact liquid core has already been

Corresponding Author: M.H. Djavareshkian, Department of Mechanical Engineering, Ferdowsi University of Mashhad, P.O. Box 91775-1111, Mashhad, Iran Tel: +98-914-3135532 Fax: +98-511-8763304

significantly disintegrated due to primary break-up mechanisms. Finally, even at the spray axis high aerodynamic break-up rates can be identified, indicating complete fragmentation of the compact spray core (Naber and Reitz, 1988).

The present study provides an overview of the proper boundary conditions and models required for successful simulation of the spray formation/propagation characteristics in direct injected diesel engines. Individual model results are validated against selected experimental data. For all cases presented in this study the CFD code FIRE is used for simulation of the relevant injector flow and spray formation and propagation processes.

MATERIALS AND METHODS

Computational fluid dynamics simulation

Basic equations: The conservation equations are presented for the following dynamic and thermodynamic properties (FIRE v8.5 Manuals, 2006):

- Mass → Equation of continuity:

$$\frac{\partial \rho}{\partial t} = -\frac{\partial}{\partial x_j}\left(\rho U_j\right) \tag{1}$$

- Momentum (Newton's second law) → Navier-Stokes Equations:

$$\frac{D(\rho U)}{Dt} = \frac{\partial(\rho U_i)}{\partial t} + \frac{\partial(\rho U_j U_i)}{\partial x_j} = \rho g_i - \frac{\partial P}{\partial x_i} + \frac{\partial}{\partial x_j}\left[\mu\left(\frac{\partial U_i}{\partial x_j} + \frac{\partial U_j}{\partial x_i} - \frac{2}{3}\frac{\partial U_k}{\partial x_k}\delta_{ij}\right)\right] \tag{2}$$

- Energy (1st Law of Thermodynamics) → Equation of energy:

$$\frac{D(\rho H)}{Dt} = \frac{\partial(\rho H)}{\partial t} + \frac{\partial(\rho U_j H)}{\partial x_j} = \rho \dot{q}_g + \frac{\partial P}{\partial t} + \frac{\partial}{\partial x_i}\left(\tau_{ij} U_j\right) + \frac{\partial}{\partial x_j}\left(\lambda \frac{\partial T}{\partial x_j}\right) \tag{3}$$

- Concentration of species equation:

$$\frac{D(\rho C)}{Dt} = \frac{\partial(\rho C)}{\partial t} + \frac{\partial(\rho U_j C)}{\partial x_j} = \rho \dot{r} + \frac{\partial P}{\partial t} + \frac{\partial}{\partial x_j}\left(D \frac{\partial C}{\partial x_j}\right) \tag{4}$$

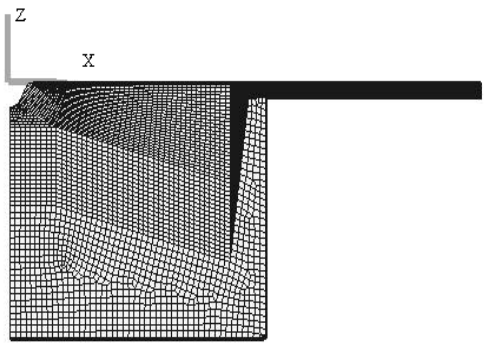

Fig. 1: Two-dimensional grid of the modeled engine

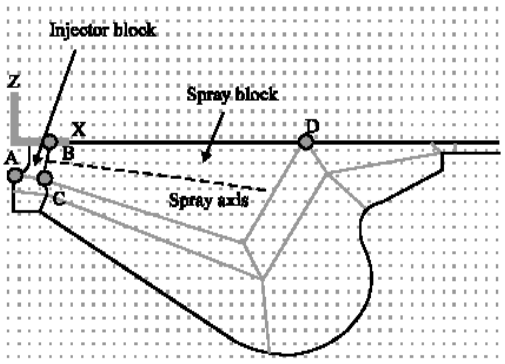

Fig. 2: Multi-block structure of the grid

Computational grid generation: Based on the geometry description, a set of computational meshes covering 360°CA is created. The mesh generation process is divided into the creation of 2D and 3D mesh. The 2D mesh of the modeled engine is shown in Fig. 1. A 90° sector mesh was used in this study considering that the diesel injector has four nozzle holes. This mesh resolution has been found to provide adequately independent grid results. The multi-block structure of the grid, containing spray and injector blocks, is shown in Fig. 2.

Overview of typical boundary conditions: The wall (surface) temperatures (cylinder liner, cylinder head and piston crown) are based on experimental experiences and depend on the operating point (load and speed). The boundary conditions of the cylinder head are specified as fixed wall, the boundary conditions of the piston bowl as moving wall. In Fig. 3, overview of the selected boundary conditions is shown.

Symmetry boundary conditions are applied to the radius surface along the center axis of the segment mesh. This symmetry boundary conditions might cause problems with calculation results regarding temperature.

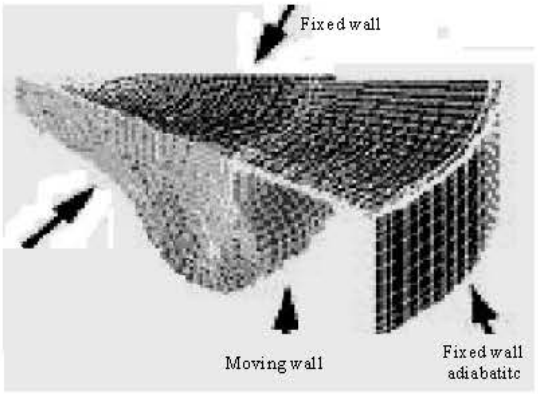

Fig. 3: Boundary conditions-overview

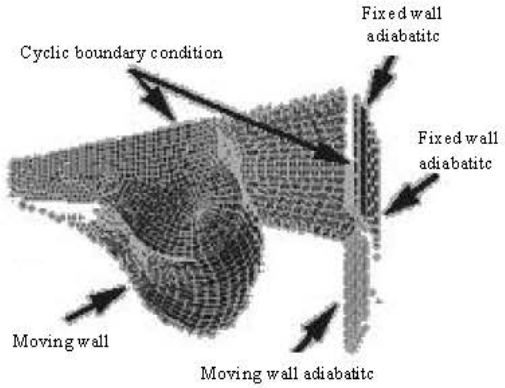

Fig. 5: Moving wall adiabatic boundary conditions

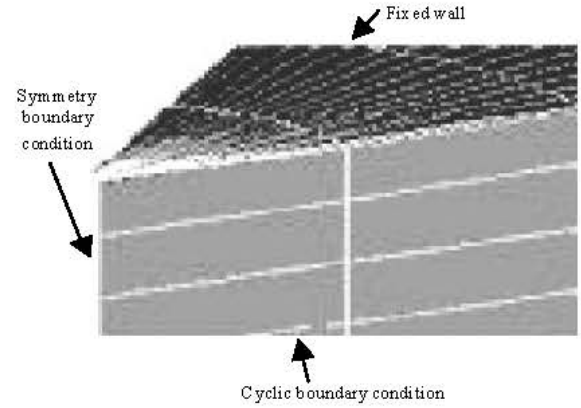

Fig. 4: Boundary conditions-details

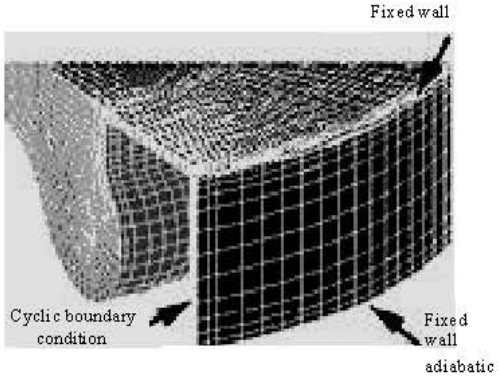

Fig. 6: Selections for cyclic boundary conditions

In this case adiabatic fixed wall boundary conditions can be specified. In Fig. 4. details of the boundary conditions is shown.

The boundary conditions concerning the additional compensation volume are applied in this way. Faces at the outer, inner and lower side of the volume are specified as moving wall adiabatic (heat flux = 0). Figure 5 shows the moving wall adiabatic boundary conditions.

The faces in polar direction are specified as cyclic boundary conditions. Figure 6 shows selections for cyclic boundary conditions.

Model formulation: The AVL FIREv8.5 CFD tool was implemented to simulate diesel engine combustion. FIRE solves unsteady compressible turbulent reacting flows by using finite volume method. Turbulent flow in the combustion chamber was modeled with k-ε turbulence model. An eddy break-up combustion model was implemented to simulate the combustion process in a diesel engine. The reaction mechanism used for the simulation of the auto-ignition of the diesel fuel is based upon an extended version of the well known SHELL model.

Auto-ignition model: The SHELL ignition model (Baumgarten, 2006) was implemented as the auto-ignition model in this study. The model uses a simplified reaction mechanism to simulate the auto-ignition of hydrocarbon fuels. The mechanism consists of eight generic reactions and five generic species. The reactions represent four types of elementary reaction steps that occur during ignition, namely, initiation, propagation, branching and termination. The five generic species include fuel, oxygen, radicals, intermediates species and branching agents. These reactions are based on the degenerate branching characteristics of hydrocarbon fuels. The premise is that degenerative branching controls the two-stage ignition and cool flame phenomena seen during hydrocarbon auto-ignition. A chain propagation cycle is formulated to describe the history of the branching agent together with one initiation and two termination reactions.

This model has been successfully applied in diesel ignition studies. It has been found that the rate-limiting step in the kinetic path is the formation of the intermediate species and the ignition delay predictions are sensitive to the pre-exponential factor A_{fj} in the rate constant of this reaction. Therefore, the above kinetic constant is adjusted to account for fuel effects.

Combustion model: The EBU model (Brink *et al*., 2000) has been developed assuming that in most technical applications the reaction rates are fast compared to the mixing. Thus, the reaction rate is determined by the rate of intermixing of fuel and oxygen-containing eddies, i.e., by dissipation rate of the eddies. For such a case, the EBU model can be written:

$$\omega = A\frac{\varepsilon}{k}\min\left(Y_{fuel}, \frac{Y_{oxygen}}{r_f}, B\frac{Y_{products}}{1+r_f}\right) \quad (5)$$

where, Y is the mass fraction and r_f the stoichiometric coefficient for the overall reaction written on mass basis. A and B are experimentally determined constants of the model, whereas k is the turbulent kinetic energy and ε its dissipation rate. The product dependence for the reaction rate is a deviation from the pure fast chemistry assumption, since the assumption here is that without products the temperature will be too low for reactions. This model assumes that in premixed turbulent flames, the reactants (fuel and oxygen) are contained in the same eddies and are separated from eddies containing hot combustion products. The chemical reactions usually have time scales that are very short compared to the characteristics of the turbulent transport processes. Thus, it can be assumed that the rate of combustion is determined by the rate of intermixing on a molecular scale of eddies containing reactants and those containing hot products, in other words by the rate of dissipation of these eddies. The attractive feature of this model is that it does not call for predictions of fluctuations of reacting species (FIRE v8.5 Manuals, 2006).

Spray and break-up modeling: Currently the most common spray description is based on the Lagrangian discrete droplet method (Burger *et al*., 2002). While, the continuous gaseous phase is described by the standard Eulerian conservation equations, the transport of the dispersed phase is calculated by tracking the trajectories of a certain number of representative parcels (particles). A parcel consists of a number of droplets and it is assumed that all the droplets within one parcel have the same physical properties and behave equally when they move, break-up, hit a wall or evaporate. The coupling between the liquid and the gaseous phases is achieved by source term exchange for mass, momentum, energy and turbulence. Various sub-models were used to account for the effects of turbulent dispersion (Barata, 2008), coalescence (Post and Abraham, 2002), evaporation (Baugmarten, 2006), wall interaction (Andreassi *et al*., 2007) and droplet break up (Liu *et al*., 2008).

Spray model equations: the differential equations for the trajectory and velocity of a particle parcel are as follows (FIRE v8.5 Manuals, 2006):
Momentum:

$$m_d\frac{dU_{id}}{dt} = F_{idr} + F_{ig} + F_{ip} + F_{ib} \quad (6)$$

Where:

F_{idr} = The drag force, given by:

$$F_{idr} = D_p \times u_{irel} \quad (7)$$

D_p = The drag function, defined as:

$$D_p = \frac{1}{2}\rho_g A_d C_D |u_{rel}| \quad (8)$$

C_D = The drag coefficient which generally is a function of the droplet Reynolds number

Re_d and A_d = The cross-sectional area of the particle

= A force including the effects of gravity and buoyancy:

$$F_{ig} = V_p\times(\rho_p-\rho_g)g_i \quad (9)$$

F_{ip} = The pressure force, given by:

$$F_{ip} = V_p \times \nabla p \quad (10)$$

F_{ib} summarizes other external forces like the so-called virtual mass force, magnetic or electrostatic forces, Magnus force or others.

Therefore, inserting above forces and relations into Eq. 6 and dividing it by the particle mass m_d the equation for the particle acceleration as used by default is:

$$\frac{du_{id}}{dt} = \frac{3}{4}C_D\frac{\rho_g}{\rho_d}\frac{1}{D_d}|u_{ig}-u_{id}|(u_{ig}-u_{id}) + \left(1-\frac{\rho_g}{\rho_d}\right)g_i \quad (11)$$

Which can be integrated to get the particle velocity and from this the instantaneous particle position vector can be determined by integrating:

$$\frac{dX_{id}}{dt} = u_{id} \quad (12)$$

Break-up modelling: The atomization of diesel engine fuel sprays can be divided into two main processes, primary and secondary break-up. The former takes place in the region close to the nozzle at high Weber numbers. It is not only determined by the interaction between the liquid and gaseous phases but also by internal nozzle phenomena like turbulence and cavitation. Atomization that occurs further downstream in the spray due to aerodynamic interaction processes and which is largely independent of the nozzle type is called secondary break-up.

The classic break-up models like TAB (Taylor Analogy Break-up), RD (Reitz and Diwakar) and WAVE do not distinguish between the two processes (Dukowicz, 1979). The parameters of these models are usually tuned to match experimental data further downstream in the region of the secondary break-up. Originally, these parameters are supposed to depend only on nozzle geometry, in reality they also account for numerical effects.

Other models like ETAB (Enhanced TAB), FIPA (Fractionnement Induit Par Acceleration) or KH-RT (Kelvin Helmholtz-Rayleigh Taylor) treat the primary break-up region separately (Dukowicz, 1979). Hence, they in principle offer the possibility to simulate both break-up processes independently. The correct values for the additional set of parameters, however, are not easy to determine due to the lack of experimental data for the primary break-up region.

Despite the sometimes tedious tuning of these model parameters the use of break-up models is generally advantageous compared to the initialization of measured droplet distributions at the nozzle orifice. In the first approach the droplets are simply initialized with a diameter equal to the nozzle orifice (blob injection), the droplet spectrum automatically evolves from the subsequent break-up processes. The latter approach gives satisfying results only as long as injection pressure and droplet Weber numbers are low (Tatschl *et al.*, 2002).

In this study we will investigate the WAVE, FIPA and KH_RT break-up models. Here, we give an overview of these models.

WAVE standard: The growth of an initial perturbation on a liquid surface is linked to its wavelength and to other physical and dynamic parameters of the injected fuel and the domain fluid (Liu and Reitz, 1993).

There are two break-up regimes, one for high velocities and one for low velocity Rayleigh type break-up. For the first case the size of the product droplets is set equal to the wavelength of the fastest growing or most probable unstable surface wave. Rayleigh type break-up produces droplets that are larger than the original parent drops. This regime is not important for high pressure injection systems.

As for the Reitz-Diwakar model also for the WAVE model a rate approach for the radius reduction of the parent drops is applied:

$$\frac{dr}{dt} = -\frac{(r - r_{stable})}{\tau_a} \tag{13}$$

where, τ_a is the break-up time of the model, which can be calculated as:

$$\tau_a = \frac{3.726 \times C_2 \times r}{\Lambda \times \Omega} \tag{14}$$

The constant C_2 corrects the characteristic break-up time and varies from one injector to another. r_{stable} is the droplet radius of the product droplet, which is proportional to the wavelength Λ of the fastest growing wave on the liquid surface:

$$r_{stable} = C_1 \Lambda \tag{15}$$

The recommended default value of C_1 taken from the original study of Reitz is 0.61. The wave length Λ and wave growth rate Ω depend on the local flow properties:

$$\Lambda = 9.02 \times r \frac{(1 + 0.45 \times Oh^{0.5})(1 + 0.4 \times T^{0.7})}{(1 + 0.87 \times We_g^{1.67})^{0.6}} \tag{16}$$

$$\Omega = \left(\frac{\rho_g r^3}{\sigma}\right)^{-0.5} \frac{0.34 + 0.38 \times We_g^{1.5}}{(1 + Oh)(1 + 1.4 \times T^{0.6})} \tag{17}$$

Entering Reynolds Re and Ohnesorge number Oh as well as $T = Oh \times We^{0.5}$.

FIPA: The researchers of this model assume that primary and secondary break-up have to be treated separately (Baritaud, 1997). As the WAVE model was developed from the analysis of perturbations on liquid surfaces it is used for primary break-up. For secondary break-up the experimentally determined equations by Pilch and Erdman (1987) are applied:

$$\begin{aligned}
\tau_{bu} &= 6.00(We - 12)^{-0.25} && 12 < We < 18 \\
\tau_{bu} &= 2.45(We - 12)^{+0.25} && 8 < We < 45 \\
\tau_{bu} &= 14.1(We - 12)^{-0.25} && 45 < We < 351 \\
\tau_{bu} &= 0.766(We - 12)^{+0.25} && 351 < We < 2670 \\
\tau_{bu} &= 5.5 && 2670 < We
\end{aligned} \tag{18}$$

τ_{bu} is the non-dimensionalized break-up time for inviscid liquids. The transition from primary to secondary break-up is arbitrarily set at We = 1000. This time the Weber number is calculated with the diameter and not with the radius. To get the break-up time τ for the secondary break-up the following relation is needed:

$$\tau = C_{23} \times \tau_{bu} \times \sqrt{\frac{\rho_l}{\rho_g}} \times \frac{d}{V_r} \quad (19)$$

The factor C_{23} is a constant similar to C_2 in the WAVE model. C_{23} is a function of the void fraction and the constants C_2 and C_3. The idea is that the break-up process is reduced in cells where the spray is densely packed. C_2 is valid for void fractions bigger than 0.99999, C_3 for void fractions less than 0.99, values in between are interpolated.

As in the WAVE model, the characteristic break-up time and the stable droplet radius control the gradual break-up process.

$$\frac{dr}{dt} = -\frac{(r - r_{stable})}{(\tau - \tau_s)^{C_6}} \quad (20)$$

Contrary to the other models there is an exponential factor C_6 and the characteristic break-up time τ is calculated only once at the beginning of the break-up. τ_s is the elapsed time since the calculation of τ.

KH-RT: In this model Kelvin-Helmholtz (KH) surface waves and Rayleigh-Taylor (RT) disturbances should be in continuous competition of breaking up the droplets (Su *et al*., 1996; Künsberg-Sarre and Tatschl, 1998).

The KH mechanism is favored by high relative velocities and high ambient density. The RT mechanism is driven by rapid deceleration of the droplets causing growth of surface waves at the droplet stagnation point. The WAVE model equations (Reitz and Bracco, 1982).

$$\begin{aligned} R_a &= C_1 \Lambda \\ \tau_a &= \frac{3.7 C_2 R}{\Lambda \Omega} \\ \Lambda &= f(We_c, Oh_d) \\ \Omega &= f(We_c, Oh_d) \end{aligned} \quad (21)$$

Simulate the KH break-up. We_c is indicating continuous phase properties and Oh_d is indicating droplet properties.

The RT disturbances are described by the fastest growing frequency Ω and the corresponding wave number K.

$$\Omega_t = \sqrt{\frac{2}{3\sqrt{3\sigma}} \frac{g_t |(\rho_d - \rho_c)|^{1.5}}{\rho_d + \rho_c}} \quad \tau_t = C_5 \frac{1}{\Omega_t} \quad (22)$$

$$K_t = \sqrt{\frac{g_t |\rho_d - \rho_c|}{3\sigma}} \quad \Lambda_t = C_4 \frac{\pi}{K_t} \quad (23)$$

Here, g is the deceleration in the direction of travel. If the wave length Λ is small enough to be growing on the droplet's surface and the characteristic RT break-up time τ has passed, the droplets atomize and their new sizes are assumed to be proportional to the RT wave length. Droplets within the break-up length L:

$$L = C_3 \sqrt{\frac{\rho_d}{\rho_c}} d_o \quad (24)$$

are considered to undergo only KH break-up, whereas further downstream both mechanisms are present. If desired also child droplets can be created by using model parameters C_6 and C_7. Parameter C_6 determines the fraction of the parcel volume which has to be detached until child parcels are initialized, while C_7 determines the fraction of the shed mass which is finally transformed into child parcels. Thus it is possible to adjust frequency by C_6 and mass of child parcels by C_7 independently. The normal velocity component given to the child parcels is calculated from disturbance wavelength and growth rate modified by model parameter C_8.

ENGINE SPECIFICATIONS AND OPERATING CONDITIONS

The OM_355 Mercedes Benz diesel engine is used in this simulation. The specifications of mentioned engine are shown in Table 1.

Equation 25 shows how the equivalence ratio in Table 1 is calculated:

$$\phi_{diesel} = \frac{(AFR)_{st}}{(AFR)_{act}} \quad (25)$$

Table 1: OM-355 engine specifications and operating conditions

Characteristics	Values
Engine model	OM-355
No. of cylinders	6
Bore	128 (mm)
Stroke	150 (mm)
Compression ratio	16.1:1
Maximum torque speed	1400 (rpm)
SOI (ATDC)	-18.5
Inlet air temp (K)	300.00
Inlet air press (kPa)	99.00
ϕ_{diesel}	0.789

RESULTS AND DISCUSSION

Figure 7 shows the comparison of mean cylinder pressure for present calculation and experimental data (Pirouzpanah, 2003). As it can be seen, the agreement between two results is very good.

One quantity characterizing the average droplet size of a spray and thus the success of spray break-up is the Sauter Mean Diameter (SMD) wich its variation with crank angle is shown in Fig. 8. If standard WAVE model with blob injection (initial droplets have the diameter of the nozzle orifice) is used for the simulation, it can be seen that the SMD has the greater value.

Figure 9 shows spray penetration for different break-up models. The penetration depth shows the temporal development of the path of the spray tip in the combustion chamber. The time-dependent development of the spray penetration length can be divided into two phases. The first phase starts at the beginning of injection (t = 0, needle begins to open) and ends at the moment the liquid jet emerging from the nozzle hole begins to disintegrate ($t = t_{break}$). Because of the small needle lift and the low mass flow at the beginning of injection, the injection velocity is small and the first jet break-up needs not always occur immediately after the liquid leaves the nozzle. During the second phase ($t \rangle t_{break}$), the spray tip consists of droplets and the tip velocity is smaller than during the first phase. The spray tip continues to penetrate into the gas due to new droplets with high kinetic energy that follow in the wake of the slower droplets at the tip (high exchange of momentum with the gas) and replace them. The spray penetration increases with time due to the effect that new droplets with high kinetic energy continuously replace the slow droplets at the spray tip.

Figure 10 presents the effect of different break-up models on the amount of liquid mass remaining after injection. The KH-RT model exhibits the most amount of liquid remaining.

Figure 11 represents mean cylinder pressure for different break-up models. Figure 11 shows that the results of the FIPA and WAVE models are close. Comparing with Fig. 8, it can be seen that smaller SMD, more surface per unit volume, more effective evaporation and mixture formation in the KH-RT model lead to higher cylinder peak pressure.

Figure 12 shows combustion rate or heat release rate for different break-up models. Figure 12 shows again the close results between FIPA and WAVE models in predicting the heat release rate. Similar to the case of

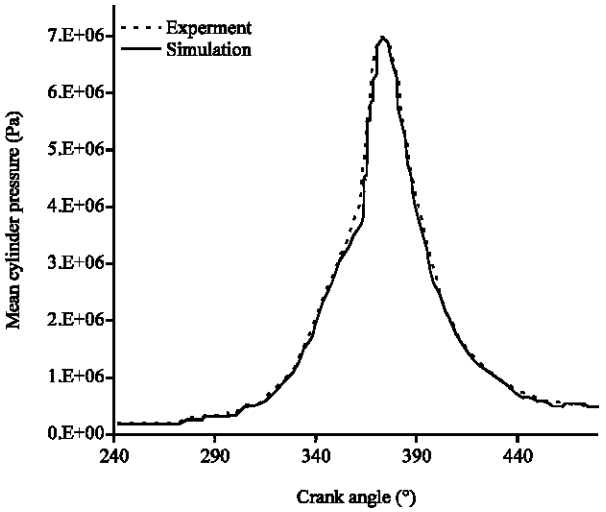

Fig. 7: Comparison of cylinder pressure for model and experiment (Pirouzpanah, 2003)

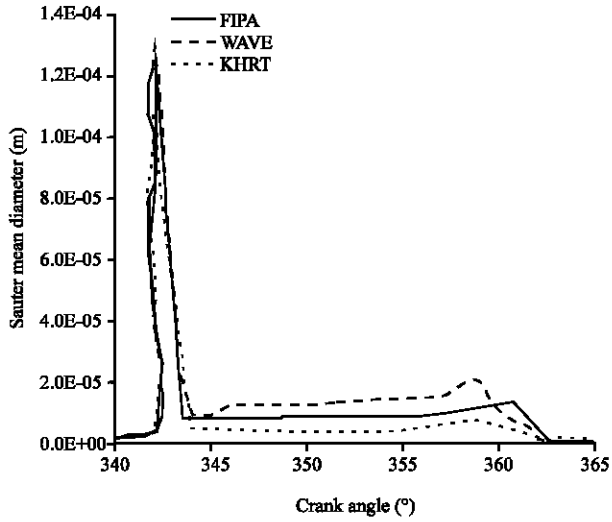

Fig. 8: Sauter mean diameter comparison for different break-up models

pressure diagrams it can be seen for KH-RT model, more effective evaporation and mixture formation, caused higher rate of heat release during the premixed phase of combustion.

Figure 13 describes the variation of the Sauter Mean Diameter (SMD) distribution during the injection process for WAVE break-up model. The growth of the simulated drops further away from the nozzle was caused by the collision and coalescence model.

It is obvious that the SMD has greater amounts near the nozzle hole and will become smaller far from the nozzle exit due to breakup process. Although the SMD is a well

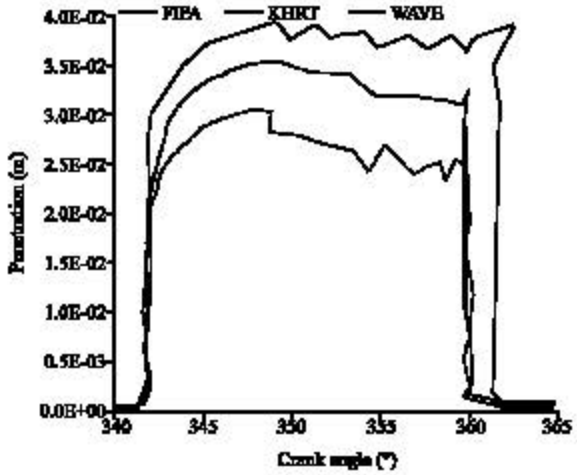

Fig. 9: Spray penetration comparison for different break-up models

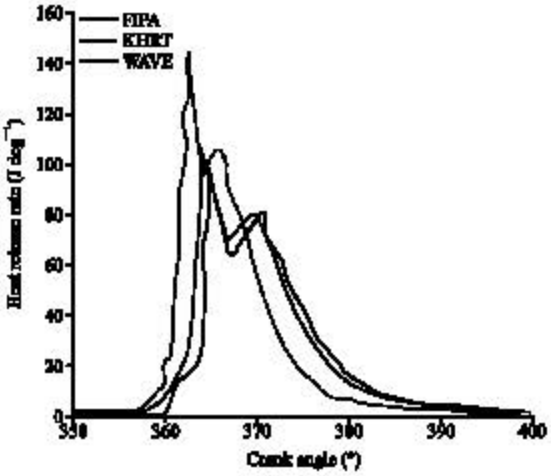

Fig. 12: Comparison of heat release rate for different breakup models

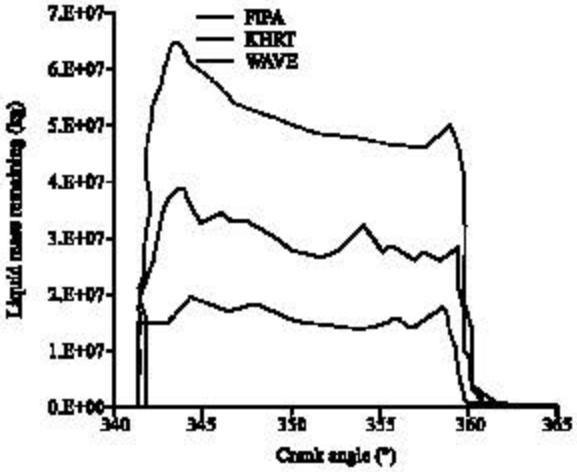

Fig. 10: Liquid mass remaining

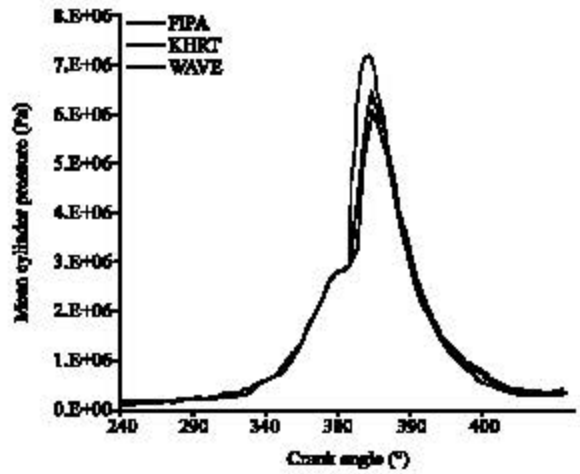

Fig. 11: Comparison of cylinder pressure for different breakup models

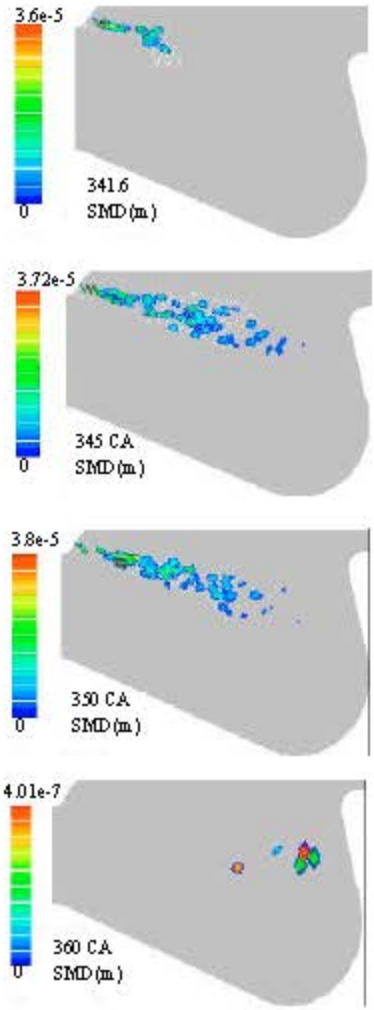

Fig. 13: Comparison of SMD in four crank angles

known quantity in characterizing the spray formation process, it is important to remember that it does not provide any information about the droplet size distribution of the spray. In other words, two sprays with equal SMD can have significantly different droplet size distributions.

CONCLUSIONS

In the present study the spray flow has been simulated with different break-up models and the effect of these models on DI diesel engine combustion and performance was investigated. All the simulations were carried out by the use of FIRE CFD tool. Results were validated with available experimental data for OM_355 DI diesel engine for mean cylinder pressure. There have been good agreements between experiments and the CFD calculations. The following conclusions may be drawn from this study:

It turns out that practically all the break-up models are capable of simulating the processes, as long as model constants are properly chosen.

The KH-RT model exhibits the most amount of liquid remaining.

For all models it can be seen that the SMD has greater amounts near the nozzle hole.

An increase in penetration can be due to reduced break-up.

Reduced penetration, increased spray disintegration and correspondingly faster fuel-air mixing causes more premixed combustion and correspondingly leads to higher cylinder peak pressure.

NOMENCLATURE

U : Velocity (m sec^{-1})
P : Pressure (Pa)
H : Enthalpy (J)
T : Temperature (K)
C : Species concentration (mol m^{-3})
k : Turbulent kinetic energy (m^2 sec^{-2})
$\dot{m}$: Mass flow rate (kg sec^{-1})
Y : Mass fraction
c : Sspecific heat (J kg^{-1} K^{-1})
r_f : Stoichiometric coefficient

Greek symbols
ρ : Density (kg m^{-3})
μ : Viscosity (kg m^{-1} sec^{-1})
ϕ : Equivalence ratio
ω : Combustion reaction rate (kmol m^{-2} sec^{-1})
ε : Turbulent dissipation rate (m^2 sec^{-3})

Subscripts
st : Stoichiometric
act : Actual

Abbreviations
DI : Direct injection
CFD : Computational fluid dynamics
CA : Crank angle
EBU : Eddy break-up
AFR : Air/fuel ratio
SOI : Start of injection
SMD : Sauter mean diameter

REFERENCES

Andreassi, L., S. Ubertini and L. Alloca, 2007. Experimental and numerical analysis of high pressure diesel spray-wall interaction. Int. J. Multiphase Flow, 33: 742-765.

Barata, J., 2008. Modeling of Biofuel droplets dispersion and evaporation. J. Renewable Energy, 33: 769-779.

Baritaud, T., 1997. Modeling atomization and break-up in high-pressure diesel sprays. SAE Trans., 106: 1391-1406.

Baumgarten, C., 2006. Mixture Formation in Internal Combustion Engines. 1st Edn., Springer-Verlag Berlin Heidelberg, New York, ISBN: 103-540-30835-0.

Brink, A., C. Mueller, P. Kilpinen and M. Hupa, 2000. Possibilities and limitations of the eddy break-up model. Combustion Flame, 123: 275-279.

Burger, M., G. Klose, G. Rottenkolber, R. Schmehl and D. Giebert *et al*., 2002. A combined eulerian and lagrangian method for prediction of evaporating sprays. J. Eng. Gas Turbines Power, 142: 481-488.

Dukowicz, J.K., 1979. Quasi-Steady Droplet Phase Change in the Presence of Convection. Los Alamos, USA.

Dukowicz, J.K., 1980. A particle-fluid numerical model for liquid sprays. J. Comput. Phys., 35: 229-253.

FIRE., 2006. Manuals AVL List GmBH. Graz, pp: 8-5.

Kunsberg-Sarre, V.C. and R. Tatschl, 1998. Spray Modelling/Atomisation-Current Status of Break-up Models. IMECHE-Seminar, The Lawn, Lincoln, UK.

Liu, A.B. and R.D. Reitz, 1993. Modeling the effects of drop drag and break-up on fuel sprays. SAE Technical paper. http://www.sae.org/technical/papers/930072.

Liu, F.S., L. Zhou, B.G. Sun, Z.J. Li and H.J. Schock, 2008. Validation and modification of wave spray model for diesel combustion simulation. Fuel, 87: 3420-3427.

Naber, J.D. and R.D. Reitz, 1988. Modeling engine spray/wall impingement. SAE 880107, 1988.

Pilch, M. and C.A. Erdman, 1987. Use of break-up time data and velocity history data to predict the maximum size of stable fragments for acceleration-induced breakup of a liquid drop. Int. J. Multiphase Flow, 13: 741-757.

Pirouzpanah, V., 2003. Reduction of pollutants emissions of OM_355 diesel engine to Euro 2 by convecting to dual fuel engine (diesel + gas). Proceedings of the 1st Conference of Conversion Automotive Fuel to CNG, Jun. 19-20, Tehran Iran, pp: 84-94.

Post, S.L. and J. Abraham, 2002. Modeling the outcome of drop-drop collisions in diesel sprays. Int. J. Multiphase Flow, 28: 997-1019.

Reitz, R.D. and F.V. Bracco, 1982. Mechanism of atomization of a liquid jet. Physics Fluids, 25: 1730-1730.

Su, T.F., M.A. Patterson, R.D. Reitz and P.V. Farrell, 1996. Experimental and numerical studies of high pressure multiple injection sprays. SAE Trans., 105: 1281-1292.

Tatschl, R. and H. Riediger, 1998. PDF modeling of stratified charge SI engine combustion. SAE Trans., 107: 1832-1841.

Tatschl, R., H. Riediger and M. Bogensperger, 1998. Multidimensional simulation of spray combustion and pollutant formation in a medium speed marine diesel engine. Proceedings of the FISITA World Automotive Congress, 1998, Paris, pp: 25-30.

Tatschl, R., H. Riediger, V.K. Sarre and N. Putz, 2000. Fast grid generation and advanced physical modelling-keys to successful application of CFD to gasoline DI engine analysis. ImechE C587/042/2000, pp: 200.

Tatschl, R., C.K. Sarre and E. Berg, 2002. IC-engine spray modeling status and outlook. Proceedings of the International Multidimensional Engine Modeling User's Group Meeting at the SAE Congress, 2002.

Ueki, H., M. Ishida and D. Sakaguchi, 2005. Investigation of droplet disintegration in diesel spray core by Advanced Laser 2-Focus velocimeter. SAE Paper No. 2005-01-1238, http://www.sae.org/technical/papers/2005-01-1238.